INFLUENCE OF AGGREGATE SIZE ON BEHAVIOR OF FRACTURE PROCESS ZONE IN CONCRETE

(Translation from Proceedings of JSCE, No.478/V-21, Nov.1993)

Koji OTSUKA

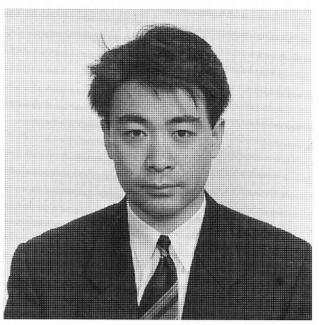

Hiroaki KATSUBE

SYNOPSIS

Experiments were carried out by an alternative x-ray technique using contrast media to investigate the internal behavior of compact tension concrete specimens. As a result, successful detection of fracture process zone consisting of numerous fine cracks forming from the tips of notches cut in the tension specimens was possible. The width of the fracture process zone increased in with larger aggregate. The fracture energy G_F calculated by the area of the fracture plane also increased with larger aggregate. The fracture energy W_F calculated by the volume of the fracture process zone was nearly constant regardless of the aggregate size.

Keywords: *fracture process zone, x-ray technique using contrast medium, internal fine cracks, fracture energy*

Koji Otsuka is a professor in the Department of Civil Engineering at Tohoku Gakuin University, Tagajo, Japan. He received his Dr. Eng. from Tohoku University in 1981. He has been involved in research on the cracking of reinforced concrete.

Hiroaki Katube is a teacher at Kurokawa High school, Miyagi, Japan. He received his Master of Engineering from Tohoku Gakuin University in 1993.

1. INTRODUCTION

Failure of reinforced concrete structures is generally caused by the cracking of concrete. Brittle failures such as diagonal shear failure, punching shear failure, torsional failure, or splitting bond failure are especially connected with crack formation. It is commonly believed that the concepts of fracture mechanics are adequate to deal with these failures caused by cracking. However, the design of concrete structures is not based on fracture mechanics because,until recently the forms of fracture mechanics available were only applicable to homogeneous brittle materials such as glass or metals, while concrete is a multiple composite material having a relatively large fracture process zone in front of crack and possessing strain-softening properties. However, the introduction of fracture mechanics into the design of reinforced concrete structures can result in significant benefits. Recently many researchers have been attempting this.

To establish the fracture mechanics of concrete, it is important to clarify the process of the failure phenomenon and the properties of the fracture process zone. Observation of the fracture process zone can be done by various means including optical microscope, electron microscope, holographic moire, laser speckle,or AE. However, except for AE, most observations are made on the concrete surface and there are therefore few studies of the properties of fracture process zones inside concrete. The authors have developed a new x-ray inspection technique using contrast medium to detect fine cracks in concrete.

The first purpose of this study was to attempt to detect fine cracks forming from the tips of notches cut in tension specimens made from concrete of different maximum aggregate size. Examing the influence of maximum aggregate size on the properties of fracture process zones was an second purpose of this study. For that purpose, fracture energy was calculated from the area and volume of the fracture process zone and the load-displacement curve.

2. MATERIALS USED IN TESTS AND TESTING METHOD

2.1 Materials and Specimens

High-early-strength Portland cement was used in the tests. Fine aggregate was a river product and coarse aggregate was either a river product or crushed stone. Maximum aggregate size (Gmax) for mortar was 5 mm. For concrete made from river product aggregate, Gmax were 10 mm, 15 mm, 20 mm, and 25 mm. For concrete made from crushed stone aggregate, Gmax were 10 mm, 15 mm, and 20 mm. The water to cement ratio of all the mixes was 0.5.

Specimens were compact tension specimens as shown in Fig. 1. A notch

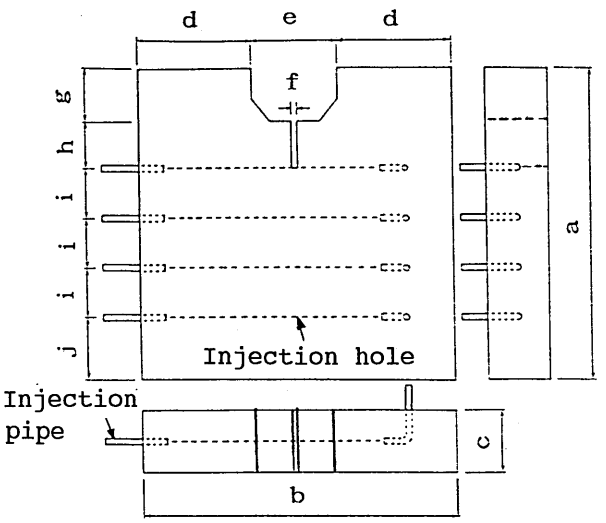

Fig. 1 Test specimen

Table 1 Dimensions of test specimens

	A type	B type
a	250	350
b	250	350
c	50	90
d	90	145
e	60	60
f	3	3
g	30	30
h	50	120
i	40	50
j	50	40

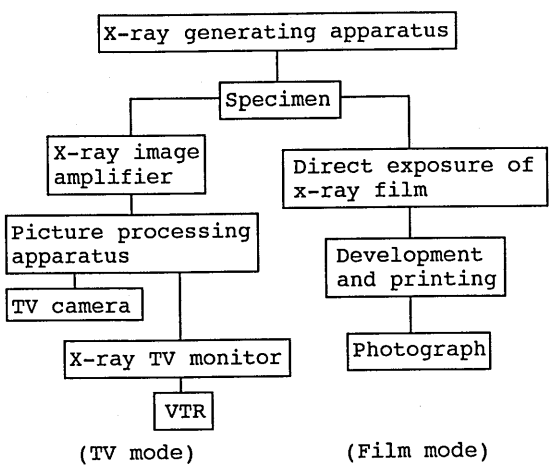

Fig. 2 Systems for detecting cracks

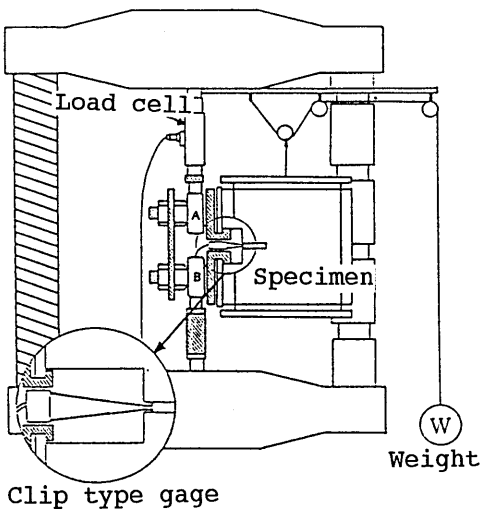

Fig. 3 Loading equipment

was cut on one side of the specimen using a diamond saw. Beforehand, small diameter holes (ID = 2 mm) were made before the concrete hardened parallel to the tension force inorder to allow injection of the contrast medium. Specimens of two types were prepared. The dimensions of A type specimens were 50 x 250 x 250 mm and of B type were 90 x 350 x 350 mm as shown in Table 1. For x-ray detection tests, 26 A type specimens (12 crushed stone aggregate and 14 river product aggregate) and 11 B type specimens (all crushed stone aggregate) were used. For fracture energy tests done by strain controlled loading, 28 A type specimens (16 crushed stone aggregate and 12 river product aggregate) were used. Specimens were cured under moist conditions until just prior to the start of each test

inorder to minimize the effects of shrinkage.

2.2 Loading Method

Figure 3 shows the loading equipment and a test specimen. A universal testing machine was used for loading. The specimen was loaded through two steel plates that were bonded to it using an adhesive agent. Half of the dead load of the specimen was canceled through the sliding wheel. A and B in the figure are hinged parts that were made to prevent additional forces to the specimen. A load cell and a clip gage were set to measure the load and the crack opening displacement.

2.3 X-ray Technique Using Contrast Medium

X-ray inspections consisted of injecting a contrast medium into the specimen's holes before loading, and performing radiography either continuously or during certain stages of loading. The systems used for detecting cracks, as shown in Fig. 2, were two kinds: A "TV mode" using an x-ray image amplifier, and a "film mode" directly exposing x-ray film. A contrast medium for the medical study of blood vessels which suited the objectives of this study was used, as was a contrast medium developed especially for this study.

In the TV mode, the distance between the x-ray generating apparatus and the specimen was fixed at 60 cm, while the distance between the specimen and image amplifier was about 30 cm. A tube voltage of 60 kv and a current of 2 mA were used. A recording was made while observing the TV monitor image in real time during loading. Interesting areas were later subjected to a high degree of picture processing inorder to obtain hard copies.

In the film mode, the distance between the specimen and the x-ray generating apparatus was 20 to 60 cm and the film was placed in close contact with the specimen. Irradiation was carried out for 3 to 20 minutes. The tube voltage was 100 kv and the current was 2 mA. The film mode has the advantage of better resolution than the TV mode, even when sophisticated TV image processing is done. This paper presents results mainly from the film mode.

3. EXPERIMENTAL RESULTS

3.1 Behavior of Fracture Process Zone

Fig. 4 shows an example of a load to crack opening displacement (COD) relationship measured from a type A specimen made from crushed stone aggregate concrete with Gmax of 20 mm. X-ray inspections were made at the numbered points on the curve.

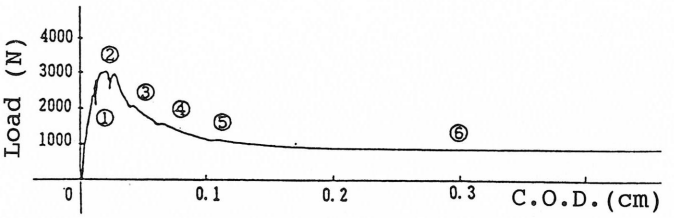

Fig. 4 Load-Crack opening displacement curve

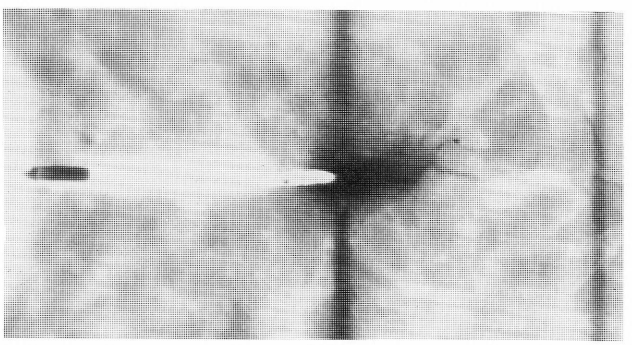

Photo 1 Result of fine crack detection by x-ray at point1

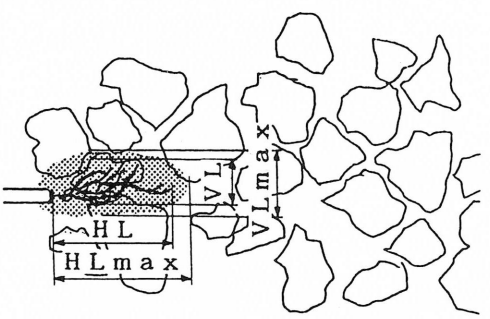

Fig. 5 Cracks traced from x-ray film at point

Photo 1 shows the result obtained at point 1 on the curve by the x-ray technique using a contrast medium. The dark parts are the cracking area where the contrast medium was injected and the longitudinal dark straight lines are injecting holes. Around cracks, gray aggregate spots can be seen, though they are not as clear as the parts injected by contrast medium. Even though the load at this time is 80% of maximum load, the photograph shows several fine cracks forming at the tip of the notch. By directly observing the x-ray film using a scharkasten, even slightly dark parts around fine cracks can be discerned as the differences in the shading of

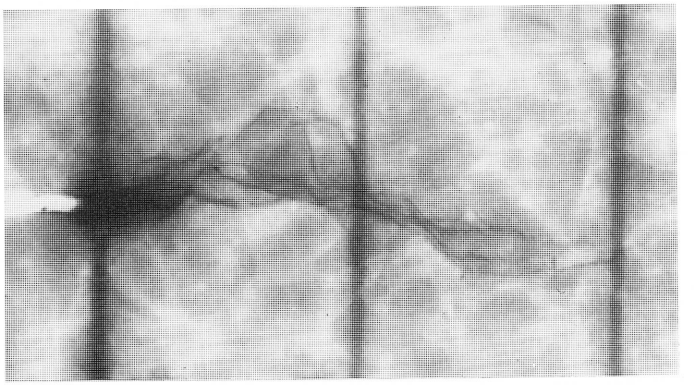

Photo 2 Results of fine cracks detection by x-ray at point 2

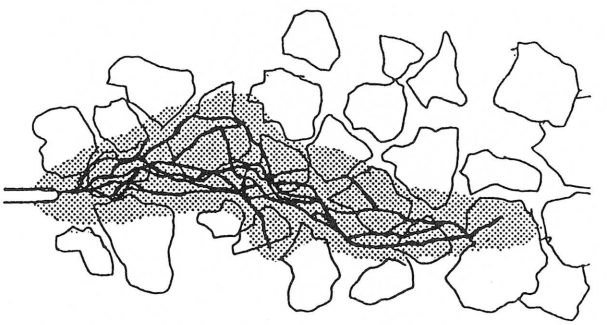

Fig. 6 Cracks traced from x-ray film at point 2

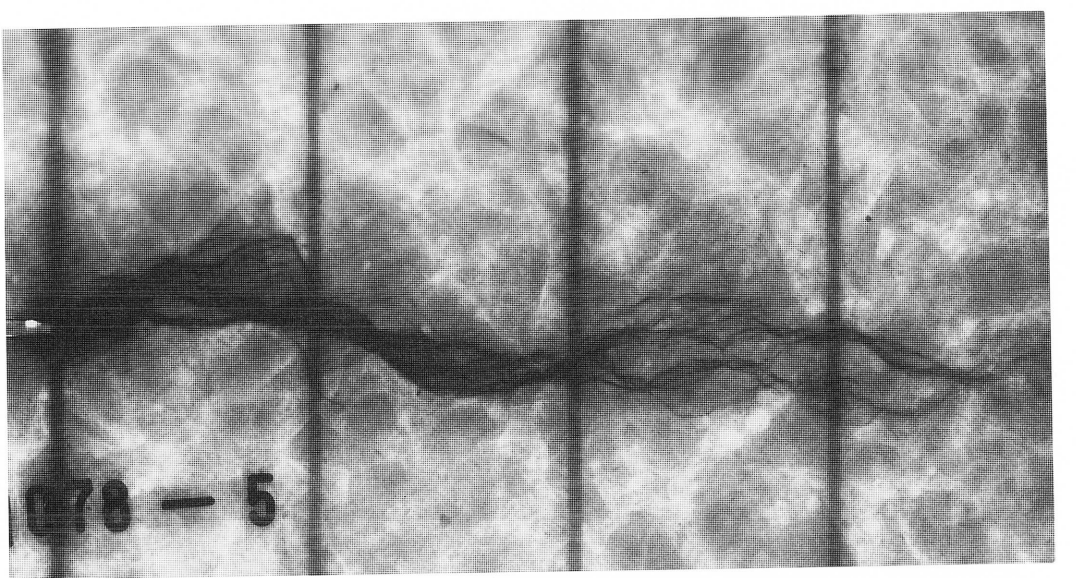

Photo 3 Results of fine cracks detection by x-ray at point 3

shadows. However,this becomes more difficult to distinguish when printed on photographic paper. It is assumed that these are additional fine micro cracks into which the contrast medium was injected. These dark cloudy parts may result from other reasons, such as fine pores in hydrated cement, and further investigation is necessary. This paper includes these dark cloudy areas in the fracture process zone.

The cracks seen through the scharkasten in Photo 1 were directly traced and are shown in Fig. 5. The netlike dark parts in the figure correspond to the cloudy dark part in the photograph. Many fine cracks in a complex configuration near the tip of the notch were detected. The horizontal (parallel to the cracking direction) length of the cracked zone (HL) was 27 mm and the maximum horizontal length of the zone of fine cracks (including the cloudy dark parts: HLmax) was 30 mm. The vertical (right angle to the cracking direction) width of the cracked zone (VL) was 7 mm. The maximum vertical width of the zone of fine cracks (including the cloudy dark parts: VLmax) was 12 mm.

Photo 2 was obtained at point 2 on the curve of Fig. 4 using an x-ray contrast medium. A large number of fine cracks radiate from the tip of the notch, as seen in Photos 1 and 2. The cracking is within a zone of certain width and length, which gradually increase as the load increases. At point 2, the load is at maximum and the values of VL and VLmax also become maximum. Fig. 6 shows the zone of fine cracks traced from the film of Photo 2. In this case, HL is 84 mm, HLmax is 92 mm, VL is 16 mm, and VLmax is 25 mm.

Photo 3 was obtained at point 5 on the curve of Fig. 4 using an x-ray contrast medium. The width of the zone of fine cracks becomes slightly narrow at the strain softening part of Fig. 4. At this point, the edges of the cracked zone reached the opposite side of the specimen. In this case, HL is 160 mm, HLmax is 170 mm, VL is 35mm, and VLmax is 45 m

3.2 Influence of Aggregate Size on Fracture Process Zone

Experiments were conducted to investigate the influence of maximum aggregate size on the configuration of the fracture process zone. For these experiments, mortar and crushed stone aggregate concrete were used to make specimens of types A B.

Fig. 7 shows four fracture process zone shapes traced from the x-ray films of four different specimens. Each was an A type specimen made from concrete with a different Gmax; 5 mm, 10 mm, 15 mm and 20 mm. The film was taken near the end of loading and cracks had grown to almost as far as the opposite side. As may be seen in these figures, the width of the process zones, VL and VLmax, differ according to Gmax, increasing with a larger Gmax. When Gmax was 5 mm, fine cracks

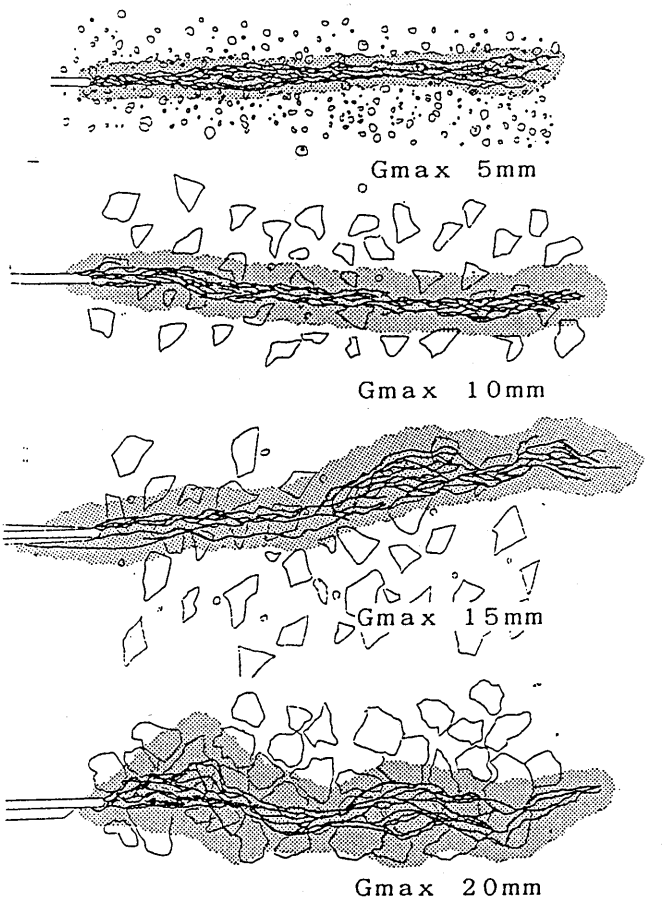

Fig. 7 Four fracture process zone shapes traced from x-ray films of four different Gmax

tended not to wander but to progress as relatively straight bundled lines. But, when Gmax was 20 mm, cracks tended to snake during their growth process, due to the presence of aggregate in the concrete.

Table 2 shows measured values of VL, VLmax, VL/Gmax, and VLmax/Gmax. Fig. 8 shows the relationships between Gmax and VL (and VLmax). It can be seen from this table and figure that as Gmax increases VL and VLmax also increase, almost linearly.The ratios of VL/Gmax and VLmax/Gmax were 2.6 and 4.0 respectively when Gmax was 5 mm. The ratio became 1.1 and 1.6 respectively when Gmax was 20 mm. A clear trend for values to become small according to Gmax increase was seen. For this reason, it may be supposed that the 50 mm width of the A type specimen was not large enough for a Gmax of 20 mm. Therefore, the experiments were done using a type B specimen with a larger thickness, 90 mm.

Table 3 shows measured value of VL, Vlmax, VL/Gmax, and Vlmax/Gmax, while fig. 9 shows the relationship between them. It can be seen

Table 2 Measured values of maximum vertical width of the zone of fine cracks (A type, Crushed stone aggregate)

Gmax (mm)	VL (mm)	VLmax (mm)	VL/Gmax	VLmax/Gmax
5	11	17	2.2	3.4
	12	12	2.4	2.4
	10	15	2.0	3.0
	19	35	3.8	7.0
average	13	20	2.5	4.0
10	9	19	0.9	1.9
	16	25	1.6	2.5
average	13	22	1.3	2.2
15	16	25	1.1	1.7
	15	24	1.0	1.6
	15	23	1.0	1.5
average	15	24	1.0	1.6
20	25	30	1.3	1.5
	14	28	0.7	1.4
	26	35	1.3	1.8
average	22	31	1.1	1.6

Table 3 Measured values of maximum vertical width of the zone of fine cracks (B type, Crushed stone aggregate)

Gmax (mm)	VL (mm)	VLmax (mm)	VL/Gmax	VLmax/Gmax
5	16	23	3.2	4.6
	13	22	2.6	4.4
	11	20	2.2	4.0
	10	20	2.0	4.0
average	13	21	2.6	4.2
10	24	35	2.4	3.5
	22	30	2.2	3.0
	22	30	2.2	3.0
average	23	32	2.3	3.2
15	20	30	1.3	2.0
	21	30	1.4	2.0
average	21	30	1.4	2.0
20	25	50	1.3	2.5
	20	45	1.0	2.3
average	23	48	1.1	2.4

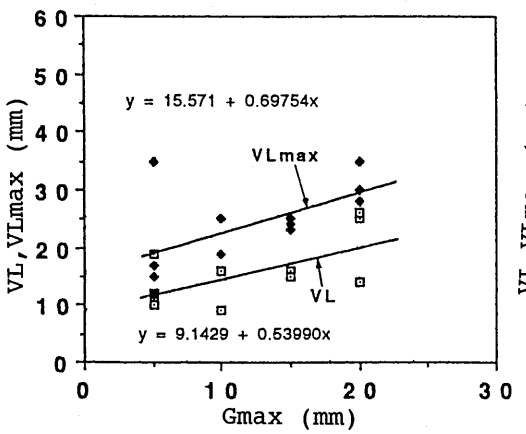

Fig.8 Relationship between Gmax and VL (and VLmax)(A type)

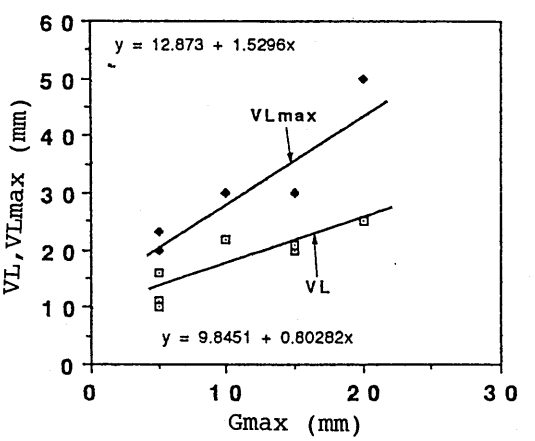

Fig.9 Relationship between Gmax and VL (and VLmax)(B type)

from these results that as Gmax increases, VL and VLmax also increase, almost linearly as in the case of the type A specimens, though the scattering of values decreases slightly. The ratio of VL/Gmax and VLmax/Gmax were 2.5 and 4.2 respectively when Gmax was 5 mm. These values are not very different from the values obtained using specimen type A (Table 2). However, when Gmax was larger than 10 mm, the ratio increased more than in the case of specimen type A and when Gmax was 20 mm, the ratio of VLmax/Gmax became 2.4. However, the value 2.4 was significantly smaller than the value 4.2 when Gmax was 5 mm. F. Wittmann concluded in his paper [4] that a width corresponding to about four times the maximum aggregate size

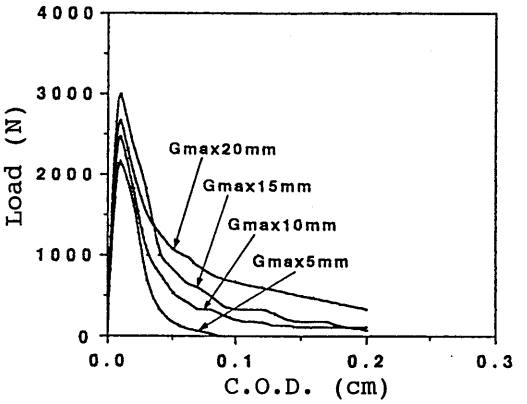

Fig. 10 Load to crack opening displacement curves

Table 4 Fracture energy G_F and W_F (A type, Crushed stone aggregate)

Gmax (mm)	σc (MPa)	G_F (N/m)	G_F average	W_F (N/m^2)	W_F average
5	30.0	64	59	53	49
	30.0	51		42	
	30.0	61		51	
	30.0	59		49	
10	30.0	93	122	62	82
	34.5	116		77	
	34.5	139		93	
	34.5	141		94	
15	33.0	149	153	76	78
	34.1	143		73	
	34.1	145		74	
	34.1	175		90	
20	36.6	176	168	80	76
	32.7	189		86	
	28.7	156		71	
	28.7	151		68	

is necessary in order to fully activate the interlocking mechanisms in the fracture process zone. However, it may be concluded from these experiments that 4 times the Gmax is not enough to do so.

3.3 Influence of Maximum Aggregate Size on Fracture Energy

Fig. 10 shows four load to crack opening displacement curves plotted in one figure. They were obtained from specimens of four Gmax, 5, 10, 15 and 20 mm. This figure shows the tendency for the slope of the curve in the softening zone to change more gently when the Gmax is larger.

Table 4 shows the fracture energy G_F calculated as the area under the load to crack opening displacement curve divided by the concrete ligament area. It can be seen from this table that G_F increases with a larger Gmax

Figure 11 shows the relationships between G_F and VL (and VLmax). From this figure, it can be seen clearly that G_F is related to the width of the fracture process zone. From these results, it is supposed that fracture energy is consumed not in the fracture plane, but in the volume of the fracture process zone. Therefore, fracture energy W_F was calculated from the area under the load versus crack opening displacement curve, divided by the volume of fracture process zone, as obtained by multiplying the average width of fracture process zone(fig. 8) by the ligament area. Table 4 shows the results of the calculation of W_F.

Fig. 12 shows the relationships between Gmax and W_F (and G_F). As can be seen in this figure, the values of W_F are nearly constant

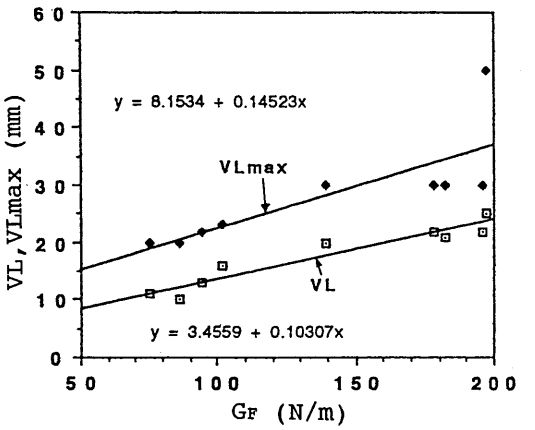

Fig.11 Relationship between G_F and VL (and VLmax)

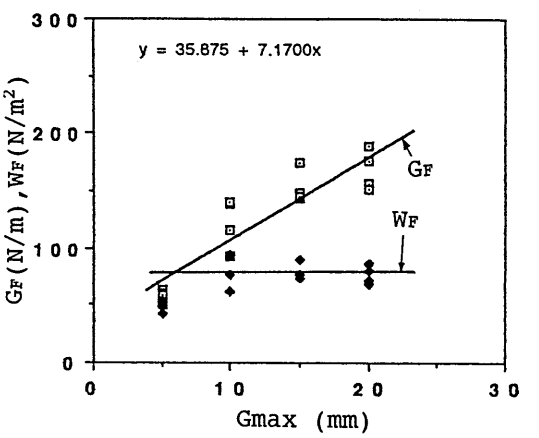

Fig.12 Relationship between Gmax and W_F (and G_F)

regardless of Gmax,with an exception at Gmax = 5 mm. The idea that the fracture energy applied to the concrete is consumed in the volume of the fracture process zone seems to be correct. It is supposed that the results of mortar were exceptional because mortar is a relatively homogeneous and brittle material with a relatively small fracture process zone width compared to concrete.

3.4 Influence of Aggregate Type on The Behavior of The Fracture Process Zone

The same experiments as presented in 3.1, 3.2, and 3.3 were carried out using concrete made of river product aggregate.

Fig. 13 shows four fracture process zone shapes traced from the x-ray films of four different specimens. Each was a type A specimen

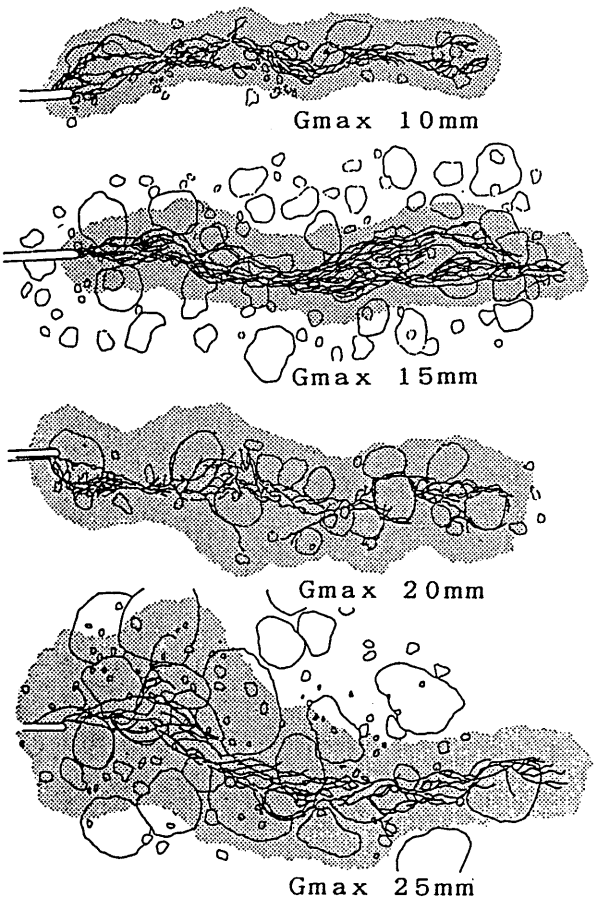

Fig. 13 Four fracture process zone shapes traced from x-ray films of four different Gmax

made from concrete of different Gmax; 10 mm, 15 mm, 20 mm, and 25 mm. All of the aggregate was river product. In the case of crushed stone aggregate (Fig. 8), many fine cracks were observed progressing through the aggregate. However, in the case of river product aggregate, cracks appear to avoid or wind around pieces of aggregate. The width of the fine crack zone, VL, also become larger than that obtained in the case of crushed stone aggregate. It may be supposed that the surface of river product aggregate is smoother than that of crushed stone aggregate and the stripping of paste from aggregate is likely to occur.

Table 5 shows measured dimensions of fracture process zones using type A specimens.The aggregate was all river product. As in the case of crushed stone aggregate, VL and VLmax increased along with Gmax. Comparing the values in Table 5 and 2 shows that the size of the fracture process zone in river product aggregate is larger than that in crushed stone aggregate.

Table 5 Result of maximum widths of the crack zones(A type, River product aggregate concrete)

Gmax (mm)	VL (mm)	VLmax (mm)	VL/Gmax	VLmax/Gmax
10	17	21	1.7	2.1
	12	35	1.2	3.5
	22	35	2.2	3.5
	12	25	1.2	2.5
average	16	29	1.6	2.9
15	19	30	1.3	2.0
	10	20	0.7	1.3
	21	30	1.4	2.0
average	17	27	1.1	1.8
20	30	40	1.5	2.0
	20	25	1.0	1.3
	35	52	1.8	2.6
	20	35	1.0	1.8
average	26	38	1.3	1.9
25	35	43	1.4	1.7
	16	30	0.6	1.2
	25	60	1.0	2.4
average	25	44	1.0	1.8

Table 6 Fracture energy G_F and W_F (A type,River product aggregate concrete)

Gmax (mm)	σc (MPa)	G_F (N/m)	G_F average	W_F (N/m^2)	W_F average
5	30.0	64	61	53	51
	30.0	61		51	
	30.0	59		49	
10	38.7	98	79	47	37
	43.7	74		35	
	43.7	65		30	
15	42.8	145	86	58	35
	32.0	53		22	
	32.0	61		25	
20	17.2	125	131	41	43
	17.2	155		52	
	40.7	113		37	
25	22.2	159	133	45	38
	45.3	103		29	
	45.3	138		39	

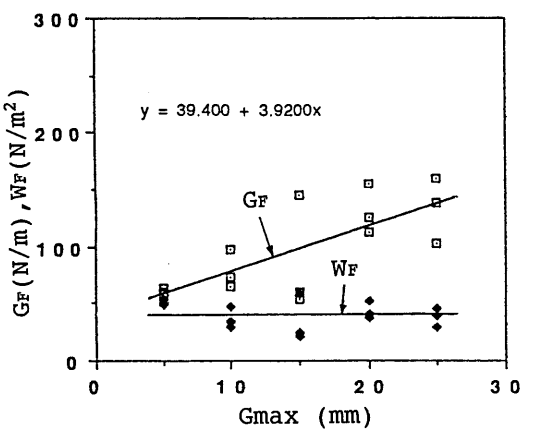

Fig. 14 Relationship between Gmax and W_F (and G_F) (River product aggregate)

Table 6 shows the fracture energies G_F and W_F, calculated by the method explained for Table 4, and Fig.14 shows their relationship, as in Figure 12. It can be seen from the table and figure that G_F increases along with Gmax, while W_F remains nearly constant, as in the case of crushed stone aggregate. However, the values of G_F and W_F are smaller than those of crushed stone, though the compressive strength of both differs only slightly. The reason is considered to

be that during the process of crack development under tensile load, cracks in crushed stone aggregate concrete are likely to penetrate the aggregate, while cracks in river product aggregate concrete avoid or wind around the aggregate. More energy may be consumed while penetrating the aggregate. This result suggests that W_F as well as G_F can be used as an index to estimate the material properties of concrete.

4. CONCLUSION

Experiments were carried out by an alternative x-ray technique using contrast media to detect fine cracks forming from the tip of a notch in compact tension specimens made from concrete of different maximum aggregate sizes. Influences of maximum aggregate size on the properties of the fracture process zone of concrete were investigated, and the following conclusions can be drawn.

(1) Through an x-ray technique using contrast media, fine cracks forming at the tip of notch in the concrete tension specimen could be detected, even at 80% of maximum load. The cracks formed a complex, intertwined network as the load increased.

(2) The vertical (right angle to the cracking direction) width of the fine crack zone achieved maximum at the maximum load and slightly decreased at the strain softening zone.

(3) After radiography, some cloudy parts around fine cracks could be observed on the x-ray film. It is believed that these parts are the fracture process zone where more fine micro cracks are forming.

(4) The vertical width of the fine crack zone increased with larger maximum aggregate size, Gmax. The maximum width was about 13 mm (2.6 times of Gmax) at Gmax = 5 mm, or about 21 mm (4.2 times of Gmax) if the cloudy zone was included. At Gmax = 20 mm, vertical width became about 23 mm (1.4 times of Gmax) and about 48 mm (2.4 times of Gmax), respectively.

(5) Fracture energy G_F (calculated as the area under the load-crack opening displacement curve divided by the concrete ligament area) increased with larger Gmax, while fracture energy W_F (calculated as the area under the load-crack opening displacement curve divided the volume of fracture process zone) was almost the same. These results seem to show that the idea that the fracture energy applied to the concrete is consumed, in average, within the hole volume of the fracture process zone is correct.

(6) Observations tended to show that width of the fine cracks zone of concrete made of river product aggregate grew larger than those of concrete made of crushed stone aggregate. A supposition was made that cracks in river product aggregate concrete avoid or wind around

pieces of aggregate, while cracks in crushed stone aggregate concrete are apt to penetrate the aggregate.

(7) Fracture energies G_F and W_F of concrete made of river product aggregate were smaller than those of concrete made of crushed stone aggregate, though the compression strength of both concrete was not so different. It is supposed that the reason stems from the differences in their behavior of crack propagation. These results suggest that W_F as well as G_F can be used as an index to estimate the material properties of concrete.

Reference

[1] Otsuka, K. : Detection of fracture process zone in concrete by means of x-ray with contrast medium, Fracture mechanics of concrete, Fram Cosl, Elsevier applied science, pp485～490, 1992.
[2] Otsuka, K. and Shoji, Y. : Detection of fracture process zone by x-ray with contrast medium, JCI colloquium on fracture mechanics of concrete structures, pp1～4, 1990.
[3] Otsuka, K. : Detection of fine cracks in reinforced concrete through x-ray techniques using contrast media, Proceedings of JSCE, No.478/V-21, pp169～178, 1992.
[4] Folker H. Wittmann : Fracture process zone and fracture energy, Fracture mechanics of concrete, Fram Cosl, Elsevier applied science, pp391～403, 1992.